

## Protective superhydrophobic coatings on the surface of anodized aluminum

A.A. Abrashov,<sup>ID</sup>\* A.I. Khafizova, N.S. Grigoryan,<sup>ID</sup> A.A. Petrushina,  
N.A. Asnis<sup>ID</sup> and T.A. Chudnova

*D. Mendeleev University of Chemical Technology of Russia, Miusskaya sq. 9, 125047  
Moscow, Russian Federation*

\*E-mail: [abrashov.a.a@muctr.ru](mailto:abrashov.a.a@muctr.ru)

### Abstract

One of the ways to protect metal surfaces from a corrosive environment that recently gained popularity is the creation of continuous surface films that feature water-repellent properties and the self-cleaning ability (the so-called superhydrophobic films). In academic and engineering publications, the term “superhydrophobic surfaces” is used for surfaces on which the contact angle of wetting with water and aqueous solutions exceeds  $150^\circ$ , a drop of water rolls off the surface when it is tilted by no more than  $10^\circ$ , and the surface exhibits a pronounced self-cleaning tendency. A known drawback of chemically produced superhydrophobic coatings (SHCs) is their low wear resistance. In this study, we examined the possibility of enhancing the wear resistance of SHC by preliminary anodic oxidation of aluminum and its alloys. An electrolyte for anodic oxidation of the surface of an AMg6 aluminum alloy containing 15 wt.%  $\text{H}_2\text{SO}_4$  and 15 wt.%  $\text{H}_3\text{PO}_4$  was developed. It was found that anodizing in the electrolyte based on sulfuric and phosphoric acids results in the formation of anodic oxide films with the required well-developed microstructured relief. It has been found that the preliminary anodizing of the aluminum surface leads to an increase in the adhesion strength with the next SHC and, consequently, to an increase in its wear resistance. Corrosion tests in a salt fog chamber showed that the developed coating withstands 830 hours in salt fog (5% NaCl) before the first centers of corrosion of the substrate appear, while the untreated aluminum alloy begins to corrode after 22 hours of exposure.

**Keywords:** *corrosion protection, surface treatment, superhydrophobic coatings, stearic acid, aluminum anodizing, hydrophobization, contact angle.*

Received: July 8, 2023. Published: August 3, 2023

doi: [10.17675/2305-6894-2023-12-3-13](https://doi.org/10.17675/2305-6894-2023-12-3-13)

### Introduction

Materials exhibiting the so-called “lotus effect” are called superhydrophobic. A manifestation of this effect is that when a water droplet contacts with such a material, it assumes a shape close to spherical, and if the material is slightly slanted with respect to the horizon, the droplet rolls down from the surface and captures all surface contaminants during its motion [1–4]. Materials are called superhydrophobic if they simultaneously feature three properties: the contact angle exceeds  $150^\circ$ , the roll-off angle does not exceed ten degrees,

and, finally, the surface self-cleaning effect occurs when water drops roll off the surface. The lotus effect or superhydrophobic surfaces are not a unique phenomenon in nature and are characteristic of many plants and insects. Water precipitating on the surface of leaves rolls down in the form of drops and, while draining from the leaf, captures dust particles with it, thus cleaning the surface of the plant [3–7]. Imparting superhydrophobic properties to a surface is used in practice to obtain anticorrosive, antifouling, or anti-icing coatings [8–19] and for the production of dirt-repellent textile materials [20]. In recent years, the creation of continuous superhydrophobic (SHP) self-cleaning films on the surface of metals is among the most popular methods for protecting metal surfaces from a corrosive environment. For example, due to the small thickness, the natural film on the surface of aluminum often does not provide reliable protection against corrosion, for example, in a humid industrial atmosphere or in sea water. Numerous studies of the possibility of imparting superhydrophobic properties to Al surface have shown that the development of stable SHP coatings can become a promising technology for corrosion protection [6, 8, 21–23], including an alternative to the process of its passivation with solutions of highly toxic Cr(VI) compounds. The preparation of a superhydrophobic surface usually includes two stages: the first stage involves the formation of a surface with microstructural roughness, followed by modification of this surface with low surface energy compounds containing long alkyls and often perfluorinated chains [3, 6, 8, 24].

To create the required surface roughness, chemical vapor deposition of ordered structures followed by treatment with hydrophobic reagents [6, 8], sol–gel technology [25–27] and laser irradiation [28, 29] are used. However, the fabrication of these micro/nanostructures usually requires special conditions, expensive materials, and complex technology, which limits the use of SHP coatings.

The anodizing process can also be used to create the necessary roughness of the aluminum surface [30, 31]. Many of the existing methods are based on the use of biologically toxic reagents, fluorosilanes, which are also rather expensive. As an alternative to the use of fluorine-containing compounds, phosphonic acids or higher carboxylic acids, such as stearic, can also be used [6, 8, 32, 33].

In this work, we study the anodic texturing of the surface of products made of Al and its alloys followed by hydrophobization in solutions based on stearic acid.

## Experimental

Aluminum AMg6 grade alloy with the following composition (in %) was selected for treatment: Al 91.1–93.68, Mg 5.8–6.8, and Mn 0.5–0.8. Samples with dimensions of 30×40×1 mm were degreased in a solution containing (g/L): Na<sub>3</sub>PO<sub>4</sub>·12H<sub>2</sub>O, 22; Na<sub>2</sub>CO<sub>3</sub>, 25; NaOH, 7.5; Na<sub>2</sub>SiO<sub>3</sub>, 10; and DS-10, 4, at 60–70°C for 10 min. The alloy surface was etched with 10% NaOH solution for 30 s at 70°C. Stearic acid was employed as the hydrophobizing agent. To dissolve stearic acid, a binary system obtained by mixing given amounts of dimethyl sulfoxide DMSO and distilled water was used. After hydrophobization, the samples were washed and dried at 80°C for 10 min.

The drop method was used for the accelerated assessment of the protective ability of conversion coatings. This is an express method that uses Akimov's solution, which contains:  $\text{CuSO}_4 \cdot 5\text{H}_2\text{O}$  82 g/L; NaCl 33 g/L; and 0.1 N HCl, 13 mL/L. The PAA (protective ability according to Akimov) of conversion coatings on aluminum or its alloys was estimated according to this method as the time (in seconds) until the color of the surface under a drop changes from gray to black [34].

The contact angle of water on aluminum plates was determined using a KRUSS DSA25 device (Germany). To operate a goniometer, pictures of drops were taken with a camera, and then the contact angle was calculated using software. Water drops with a volume of 2–5  $\mu\text{L}$  were applied to the surface of the samples, and the contact angle was first determined by measuring the slope of the tangent to the drop at the liquid/solid interface. For an accurate assessment, the water contact angle was calculated by taking measurements at 4–6 different locations on the sample. Purified water was used in all these experiments. The experiments were carried out at room temperature ( $\sim 25^\circ\text{C}$ ) and at constant air humidity ( $\sim 60\%$ ).

The same goniometer was also used to determine the drop roll-off angle.

Corrosion tests were carried out in an Ascott S450iP salt fog chamber (UK) in accordance with ASTM B117 standard. 5% NaCl (pH 6.5–7.2) salt solution was used, which was sprayed inside the chamber with the test samples. The temperature in the chamber was  $35^\circ\text{C}$  and the humidity was 95–100%. Inspection of the samples was carried out 3 times a day to detect the appearance of the first corrosion spots.

The surface topography of the samples with the coatings in question was studied using a 3D optical profilometer (SuperView W1, CHOTEST, China). The profilometer was configured in the scanning phase-shifting interferometer mode, the declared resolution along the Z axis was 0.1 nm, and the measurement accuracy was 0.7%. Profilometers of this type include an interferometer with a reference plate installed in one arm and the sample under study in the other. To measure the path difference of the interfering rays, the interference pattern was modeled and converted into a photoelectric signal, after which information about the surface profile was extracted from the phase component of the detected signal. Monochromatic radiation generated by a green LED was used to obtain the interference pattern.

To determine the features of the relief (morphology) of the surface of the conversion coatings formed on aluminum samples, the surface was photographed with a scanning electron microscope (Thermo Fisher Scientific Quattro C) equipped with an Everhart and Thornley R580 SE secondary electron detector at an accelerating voltage of 10 kV, a probe current of 0.18–3 nA, an aperture size of 20  $\mu\text{m}$ , and a focal length of 10 mm in high vacuum. The sample was located perpendicular to the incident electron beam, and the detector was tilted with respect to the surface being studied. The object was photographed with a magnification of 10000 with a 25 cm diagonal length of the raster image on the monitor.

Polarization measurements were carried out using an Autolab PGT302N potentiostat in potentiodynamic mode at a scanning rate of 0.5 mV/s. Samples of galvanized steel with

coatings being developed were used as the working electrodes. The electrode potentials were measured relative to the silver chloride electrode, and their values were converted to the normal hydrogen scale.

The Tafel extrapolation method was used to determine the values of the corrosion potential ( $E_{\text{corr}}$ ) and corrosion current density ( $i_{\text{corr}}$ ) [35]. The  $E_{\text{corr}}$  and  $i_{\text{corr}}$  values were determined from the coordinates of the intersection points of the extrapolated anodic and cathodic Tafel portions of the voltammograms.

The mechanical durability of the surface of samples with a protective coating was tested according to the ASTM F735 standard [36]. The sample fixed at the bottom of a container was covered with a 20-mm high layer of calibrated sand (fraction from 500 to 800  $\mu\text{m}$ ). The container with sand was placed on the platform of an SHO-1D orbital shaker (Daihan, South Korea), which oscillated with a frequency of 300  $\text{min}^{-1}$ . The forces of inertia cause the entire mass of sand to move inside the container and exert a significant abrasive effect on the surface of the sample fixed at the bottom of the container.

The specific pore surface area and porosity of the studied coatings were calculated from the low-temperature nitrogen adsorption-desorption isotherms obtained using a NOVA 600 gas sorption analyzer (Anton Paar GmbH, Austria). The specific surface area ( $S_{\text{sp}}$ ) of the samples was calculated by the BET (Brunauer–Emmett–Teller) method using the adsorption branch of the isotherm in the range of relative pressures ( $p/p_0$ ) 0–0.35. The volume ( $V_p$ ) and diameter ( $d_p$ ) of the pores were calculated by the BJH (Barrett–Joyner–Halend) method from the desorption branch of the isotherm.

## Results and Discussion

The process of making the surface a superhydrophobic one usually consists of two stages: the first one is the creation of a microrough structure on the surface, while the second stage is the modification of the created microrough surface by adsorption of compounds containing long alkyl chains with low surface energy.

A solution containing dimethyl sulfoxide and water in 7:1 ratio and stearic acid in an amount of 3 g/L was used as the object of the study. It makes it possible to form, at  $t=30^\circ\text{C}$  and  $\tau=10$  min, superhydrophobic coatings (SHCs) with a contact angle of  $160^\circ$  [37, 38].

In treating the surface of AMg6 alloy with a solution of stearic acid in the binary DMSO/H<sub>2</sub>O solvent system, it can be assumed that aluminum stearate is predominantly formed on the surface, which is ultimately responsible for the hydrophobization effect achieved. Probably, the formation of a hydrophobic coating results from the sequence of stages shown in Figure 1 [37].

A microrough structure can be created on the surface in several ways: by etching, laser processing, anodic oxidation, etc. In this work, the effect of the parameters of anodic oxidation of AMg6 alloy on the properties of the finishing superhydrophobic coating was studied.

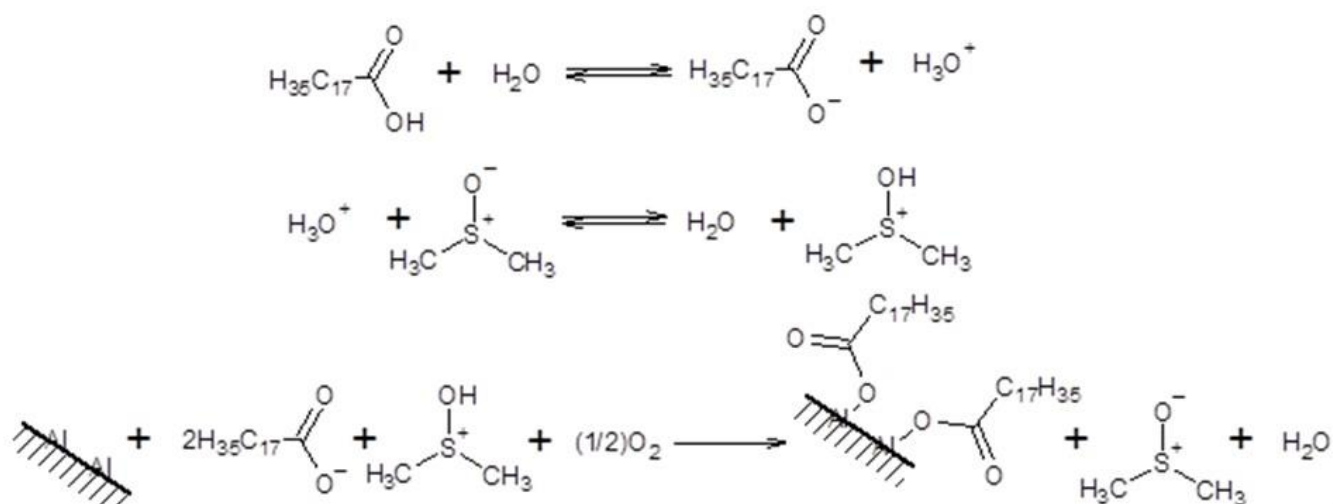


**Figure 1.** Scheme of the formation of a superhydrophobic coating.

A solution containing 15 wt.% sulfuric acid was chosen as the electrolyte. Anodizing in this electrolyte was carried out for 20 min at a temperature of 25°C, the voltage on the bath being 12 V. It was found that the subsequent hydrophobization of the aluminum surface anodized in a sulfuric acid solution results in a coating with a high protective ability (PAA)=65 min. Despite the high protective ability, the contact angle of the surface was only 125°, while the roll-off angle was 60° (Table 1).

**Table 1.** Composition of anodizing solutions and characteristics of coatings.

H <sub>2</sub> SO <sub>4</sub> concentration in the anodizing electrolyte, wt.%	H <sub>3</sub> PO <sub>4</sub> concentration in the anodizing electrolyte, wt.%	Θ, deg	Roll-off angle, deg	PAA, min	Roughness, μm	
					R <sub>a</sub>	R <sub>z</sub>
15	0	125	60	65	0.16	0.82
	5	143	20	76	0.73	5.04
	10	162	8	70	0.4	3.28
	15	164	6	60	0.54	3.85
	20	158	9	35	0.45	3.68

The isotherms of low-temperature nitrogen adsorption-desorption obtained using a NOVA 600 gas sorption analyzer made it possible to calculate the specific surface area and porosity of the oxide coatings (Figure 2).

It has been found that the pore diameter of the oxide coating obtained from the sulfuric acid electrolyte is predominantly in the range of 6.6–12.5 nm. The specific pore area ( $S_{sp}$ ) is 1.37 m<sup>2</sup>/g. With an increase in the H<sub>3</sub>PO<sub>4</sub> concentration in the sulfuric acid electrolyte, the

specific pore area decreases and formation of larger pores begins. The layers formed in the 15 wt.%  $\text{H}_2\text{SO}_4$ +15 wt.%  $\text{H}_3\text{PO}_4$  solution in 15 min at a temperature of  $35^\circ\text{C}$  and a voltage of 12 V show the highest protective ability (Table 1). The surface of anodized aluminum mainly contains pores with a diameter of 17.7–30.9 nm and a specific area of  $0.15\text{ m}^2/\text{g}$ .

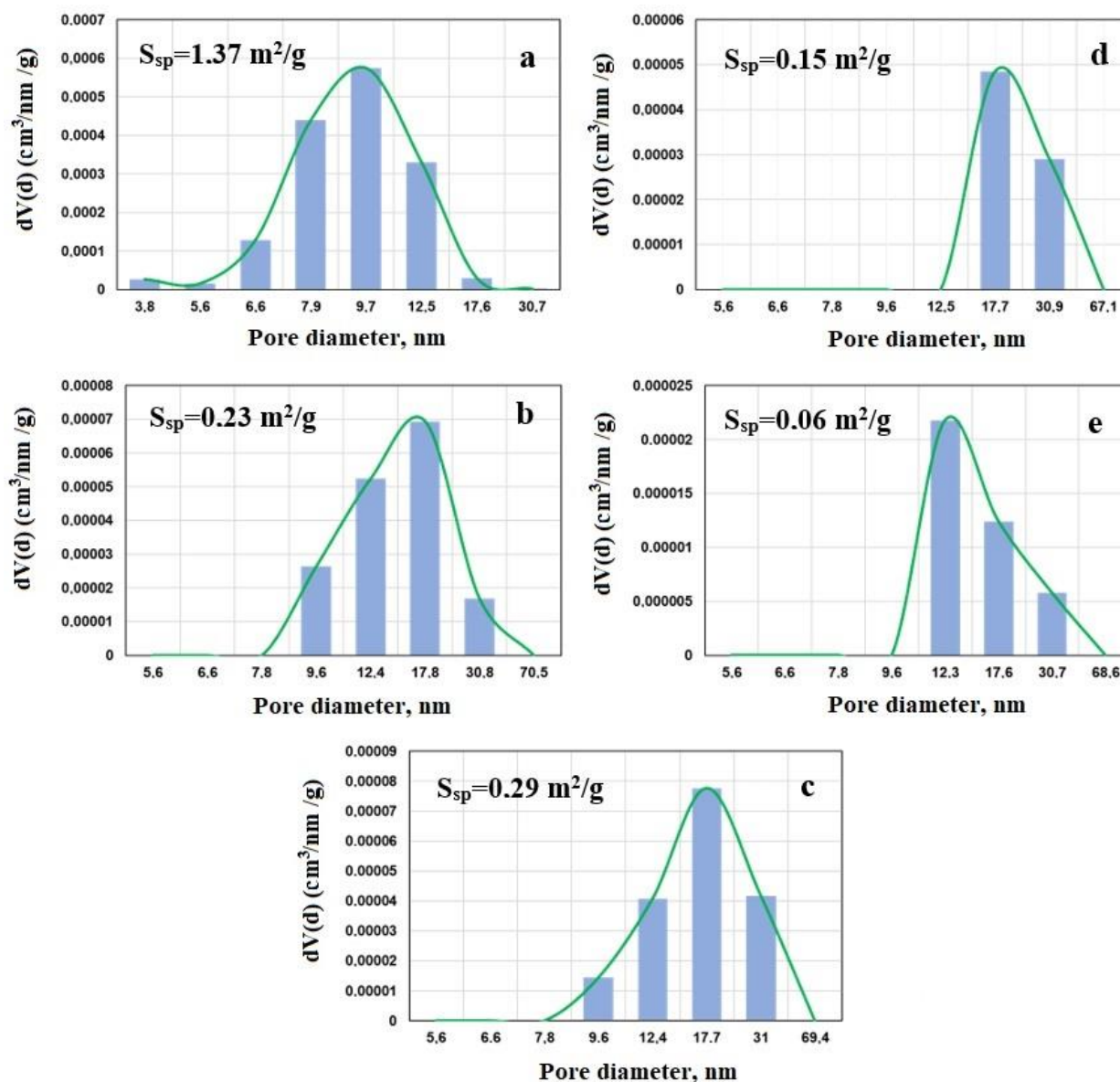


**Figure 2.** Pore distribution over the surface of anodized aluminum. Anodizing solutions: a – 15%  $\text{H}_2\text{SO}_4$ ; b – 15%  $\text{H}_2\text{SO}_4$ +5%  $\text{H}_3\text{PO}_4$ ; c – 15%  $\text{H}_2\text{SO}_4$ +10%  $\text{H}_3\text{PO}_4$ ; d – 15%  $\text{H}_2\text{SO}_4$ +15%  $\text{H}_3\text{PO}_4$ ; e – 15%  $\text{H}_2\text{SO}_4$ +20%  $\text{H}_3\text{PO}_4$ .

The photographs obtained using a scanning electron microscope made it possible to determine that the coatings obtained from the 15 wt.%  $\text{H}_2\text{SO}_4$ +15 wt.%  $\text{H}_3\text{PO}_4$  solution followed by hydrophobization have a uniform structure on the entire surface (Figure 3). The maximum contact angle of the surface is  $168^\circ$ , and the roll-off angle is  $6^\circ$ . For comparison, the roll-off angle for the non-hydrophobized alloy exceeds  $100^\circ$ .



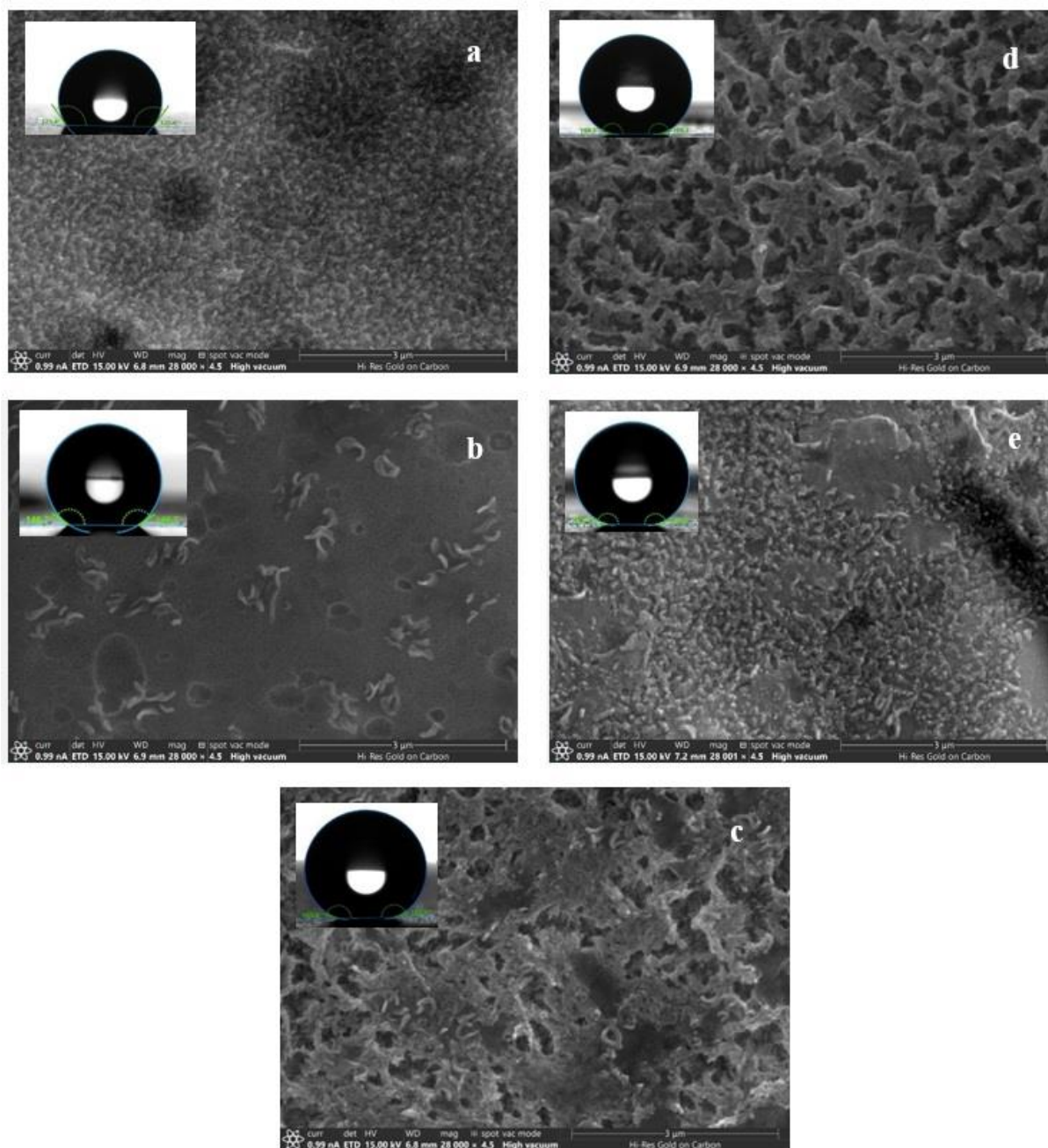


**Figure 3.** Images of the surface of anodized aluminum ( $\times 28000$ ). Anodizing solutions: a – 15%  $\text{H}_2\text{SO}_4$ ; b – 15%  $\text{H}_2\text{SO}_4$ +5%  $\text{H}_3\text{PO}_4$ ; c – 15%  $\text{H}_2\text{SO}_4$ +10%  $\text{H}_3\text{PO}_4$ ; d – 15%  $\text{H}_2\text{SO}_4$ +15%  $\text{H}_3\text{PO}_4$ ; e – 15%  $\text{H}_2\text{SO}_4$ +20%  $\text{H}_3\text{PO}_4$ .

It is known that the surface morphology of anodized aluminum is affected by the bath voltage. Therefore, we studied the effect of voltage on the characteristics of superhydrophobic layers (Table 2). The experimental data obtained made it possible to determine that the optimal voltage of the anodizing process in this electrolyte for obtaining a superhydrophobic coating is 12 V.

**Table 2.** Dependence of the characteristics of the superhydrophobic coating on the bath voltage used for anodizing.

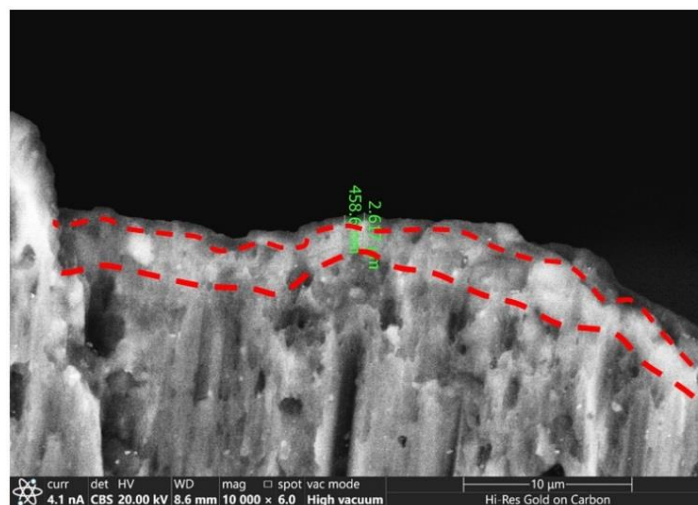
Voltage	$\Theta$ , deg	Roll-off angle, deg
10	166	7
11	160	15
12	168	7
13	164	10
14	166	7

The effect of the duration of the treatment in a solution of stearic acid on the characteristics of the resulting coatings was studied. It was shown that if the duration of hydrophobization is increased to 10 min, the contact angle of the surface of the resulting coating increases to 168°.

The effect of the concentration of stearic acid on the characteristics of the resulting coatings was studied. It was found that to improve the contact angle, a solution containing 3–4 g/L of stearic acid should be used.

Thus, to make the surface of anodized aluminum hydrophobic, it is recommended to use a solution containing 3–4 g/L of stearic acid and the following process parameters:  $t=30^{\circ}\text{C}$ ,  $\tau=10$  min, with stirring.

Scanning microscopy of cross-sections was used to determine the thickness of the anodic oxide and the superhydrophobic layers formed on the aluminum surface. It was found that the thickness of the oxide layer formed after 15 min of anodization was 0.46  $\mu\text{m}$ , while the thickness of the upper superhydrophobic coating was 2.617  $\mu\text{m}$  (Figure 4).

**Figure 4.** Photo of a microsection of an anodized aluminum sample with a superhydrophobic coating ( $\times 10000$ ).



The wear resistance of the coatings being developed was studied in comparison with superhydrophobic coatings obtained by a technology that involves a preliminary etching stage. It has been found that the superhydrophobic coating on the aluminum surface loses its superhydrophobic properties after 15 min of the sand resistance test. Superhydrophobic coatings formed on anodized aluminum show greater wear resistance. The coating maintains superhydrophobic properties even after 20 hours of testing (Figure 5). The protective ability is reduced from 60 to 45 minutes. The coating ceases to be superhydrophobic after 22 hours of testing, though it is not erased completely.

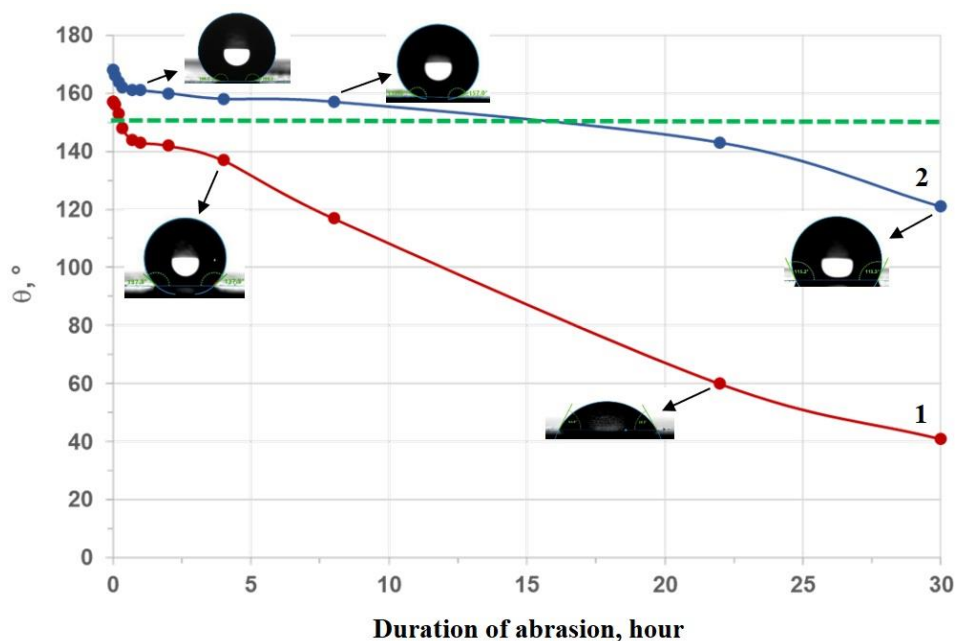


**Figure 5.** Dependence of the contact angle on the duration of abrasion. 1 – etching+SHP; 2 – anodizing+SHP.

Corrosion testing of samples of aluminum alloy AMg6 with oxide oxidation and a hydrophobic coating in a salt fog chamber showed that the developed coating withstands 830 h in salt fog (5% NaCl) until the first corrosion sites appear on the metal, while the untreated alloy begins to corrode after 22 h (Figure 6).

The data obtained correlate with the results of electrochemical studies (Table 3). The corrosion rate of anodized aluminum after superhydrophobization calculated using the Evans diagram is  $5.5 \cdot 10^{-10}$  A/cm<sup>2</sup> and is smaller than the corrosion rate of the aluminum anodized in a sulfuric acid solution followed by thickening in hot water or in a solution for aluminum chromating.

The results of corrosion tests also indicate that even if the coating loses superhydrophobic properties, it continues to provide strong protection of the alloy against corrosion: the appearance of the first corrosion site of the metal on the sample is only observed after 830 h of testing.

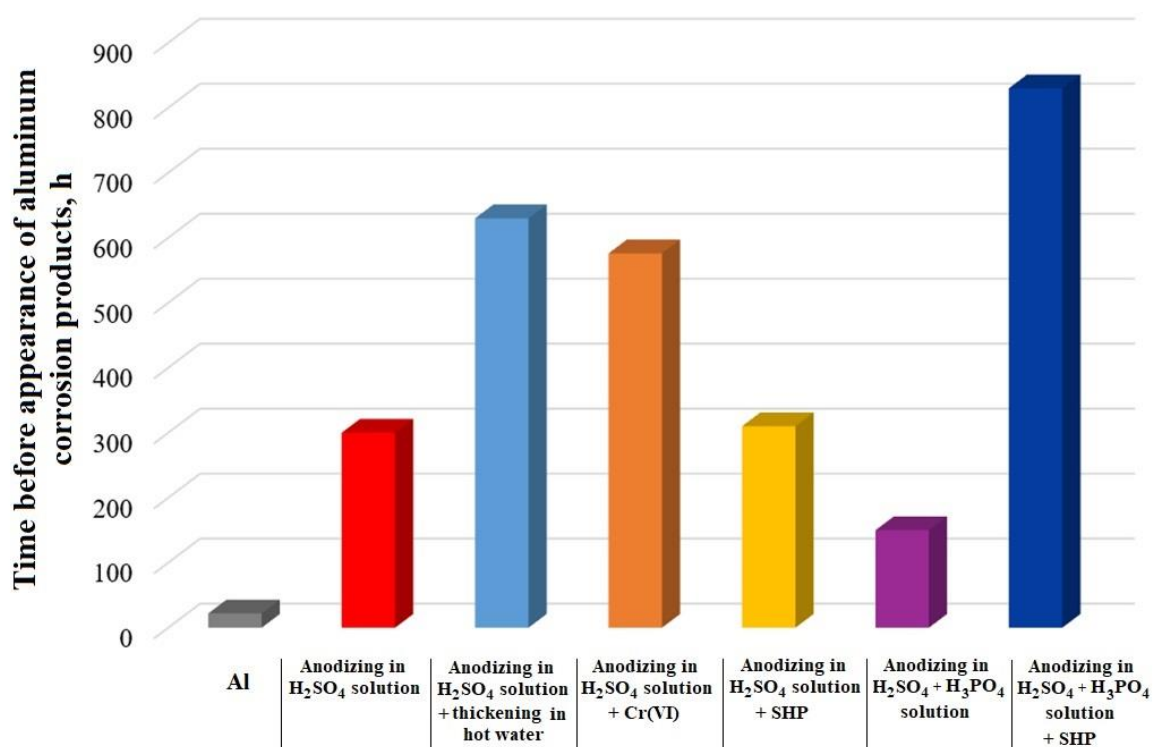


**Figure 6.** Results of corrosion tests in a salt fog chamber.

**Table 3.** Results of electrochemical studies.

Treatment type	$E_{\text{corr}}$ , V (SHE)	$i_{\text{corr}}$ , A/cm <sup>2</sup>	$K_p$ , mm/year
Al without processing	-0.7	$5.9 \cdot 10^{-7}$	0.019
Al with hydrophobization	-0.6	$2.1 \cdot 10^{-6}$	0.069
Anodizing in H <sub>2</sub> SO <sub>4</sub>	-0.5	$1.24 \cdot 10^{-8}$	0.00041
Anodizing in H <sub>2</sub> SO <sub>4</sub> followed by thickening in water	-0.76	$5.3 \cdot 10^{-9}$	0.00017
Anodizing in H <sub>2</sub> SO <sub>4</sub> followed by chromatizing	-0.64	$1.7 \cdot 10^{-9}$	$5.6 \cdot 10^{-5}$
Anodizing in H <sub>2</sub> SO <sub>4</sub> +H <sub>3</sub> PO <sub>4</sub>	-0.45	$8.5 \cdot 10^{-9}$	0.00028
Anodizing in H <sub>2</sub> SO <sub>4</sub> +H <sub>3</sub> PO <sub>4</sub> followed by hydrophobization	-0.34	$5.5 \cdot 10^{-10}$	$1.8 \cdot 10^{-5}$

It is known that the parameter of a hydrophobic coating that determines its self-cleaning ability is the roll-off angle of a water drop from its surface. If the roll-off angle is large, self-cleaning of the surface is hindered and the corrosion resistance of the coating deteriorates.

We studied the variation in the contact angle of the surface of hydrophobized anodized samples as a function of the duration of their exposure in a salt fog chamber. The results displayed in Figure 7 show that after 50 h of exposure, the surface retains superhydrophobic

properties, but after 100 h the contact angle decreases to  $117^\circ$ , which indicates the degradation of the protective coating.

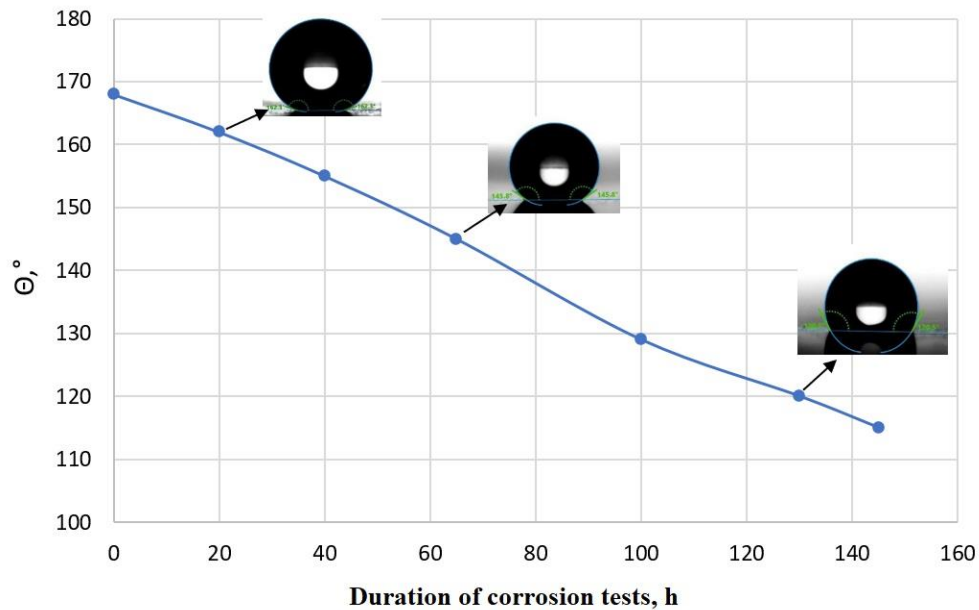


**Figure 7.** Contact angle of the surface as a function of the duration of corrosion tests in a salt fog chamber.

In this study, we examined not only the roll-off angles, but also the self-cleaning tendency. The tests for removal of graphite powder from the surface are shown in Figure 8.

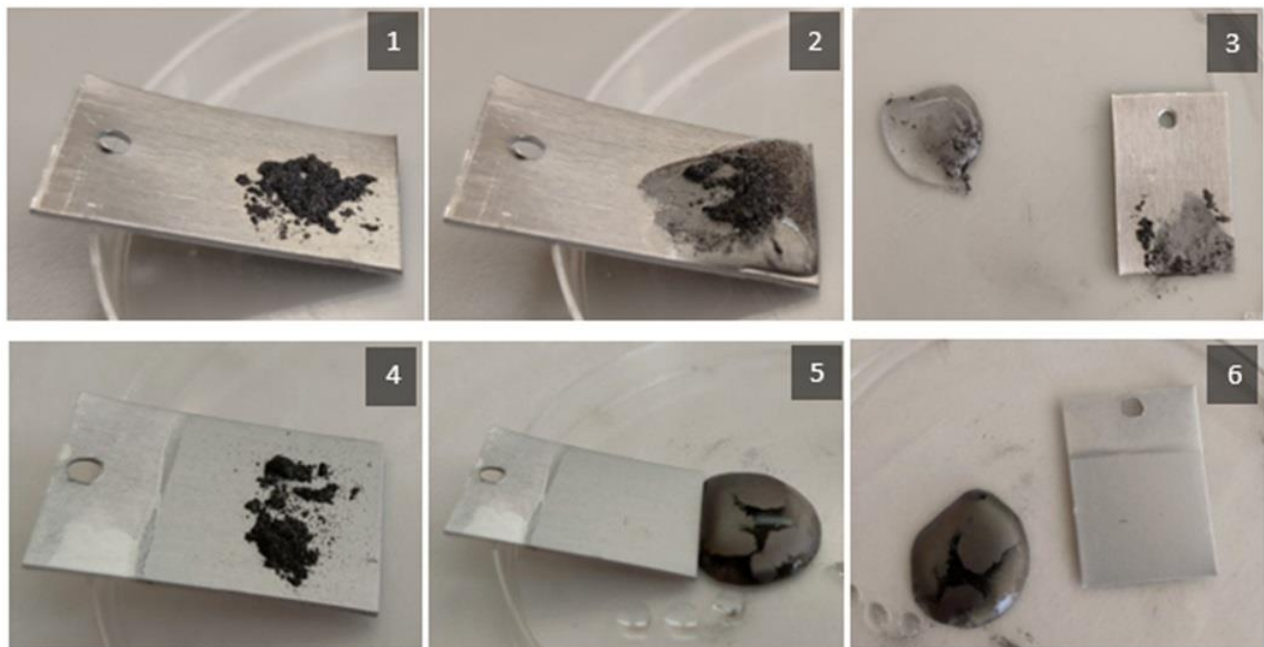


**Figure 8.** Test of the self-cleaning capability: (1–3) AMg6 aluminum alloy substrate; (4–6) AMg6+anodizing+superhydrophobic coating.

The test samples were sprinkled with GK-3 graphite powder with a particle size less than 6  $\mu\text{m}$  and placed at an angle of  $5^\circ$ . Drops of water were applied continuously to remove contaminants. Once the drops rolled off, carbon black remained on the samples of non-hydrophobized aluminum alloy. On the sample that was previously anodized and a superhydrophobic coating was applied on it (Figure 8 d, e, f), water drops bounced off the surface, carrying the simulated contaminants with them, which indicates a good ability to self-clean the surface from contaminants.

## Conclusions

As a result of the studies, an electrolyte was developed for anodic oxidation of the surface of an AMg6 aluminum alloy, which contained 15 wt.%  $\text{H}_2\text{SO}_4$  and 15 wt.%  $\text{H}_3\text{PO}_4$ . It was found that anodizing in the electrolyte based on sulfuric and phosphoric acids resulted in the formation of anodic oxide films with a well-developed microstructured relief.

It was found that the samples that were subjected to anodic oxidation exhibited the best resistance to abrasion. Such a coating lost its superhydrophobic properties after 20 hours of abrasion, whereas a superhydrophobic coating lost superhydrophobic properties after 20 minutes.

It was found that an increase in the concentration of stearic acid in the hydrophobizing solution to 4 g/L led to a significant increase in the contact angle of the surface up to  $170^\circ$ .

Corrosion testing (ASTM B117) in a salt fog chamber showed that the developed coating withstood 830 hours under salt fog conditions (5% NaCl) before the first corrosion sites appeared on the metal, while the untreated aluminum alloy began to corrode after 22 hours of exposure.

## References

1. H.Y. Erbil, Practical applications of superhydrophobic materials and coatings: problems and perspectives, *Langmuir*, 2020, **36**, 2493–2509. doi: [10.1021/acs.langmuir.9b03908](https://doi.org/10.1021/acs.langmuir.9b03908)
2. J.T. Simpson, S.R. Hunter and T. Aytug, Superhydrophobic materials and coatings: A review, *Rep. Prog. Phys.*, 2015, **78**, 086501. doi: [10.1088/0034-4885/78/8/086501](https://doi.org/10.1088/0034-4885/78/8/086501)
3. J. Jeevahan, M. Chandrasekaran, B.G. Joseph, R.B. Durairaj and G. Mageshwaran, Superhydrophobic surfaces: a review on fundamentals, applications, and challenges, *J. Coat. Technol. Res.*, 2018, **15**, 231–250. doi: [10.1007/s11998-017-0011-x](https://doi.org/10.1007/s11998-017-0011-x)
4. L.B. Boinovich and A.M. Emelyanenko, Hydrophobic materials and coatings: principles of design, properties and applications, *Russ. Chem. Rev.*, 2008, **77**, no. 7, 583–600. doi: [10.1070/RC2008v077n07ABEH003775](https://doi.org/10.1070/RC2008v077n07ABEH003775)
5. L.B. Boinovich, A.M. Emelyanenko, A.D. Modestov, A.G. Domantovsky and K.A. Emelyanenko, Not simply repel water: The diversified nature of corrosion protection by superhydrophobic coatings, *Mendeleev Commun.*, 2017, **27**, no. 3, 254–256. doi: [10.1016/j.mencom.2017.05.012](https://doi.org/10.1016/j.mencom.2017.05.012)

6. D. Zang, R. Zhu, W. Zhang, J. Wu, X. Yu and Y. Zhang, Stearic acid modified aluminum surfaces with controlled wetting properties and corrosion resistance, *Corros. Sci.*, 2014, **83**, 86–93. doi: [10.1016/j.corsci.2014.02.003](https://doi.org/10.1016/j.corsci.2014.02.003)
7. J.W. Drelich, L. Boinovich, E. Chibowski, C. Della Volpe, L. Hołysz, A. Marmur and S. Siboni, Contact angles: History of over 200 years of open questions, *Surf. Innovations*, 2020, **8**, no. 1–2, 1–25.
8. Y.I. Kuznetsov, A.M. Semiletov, A.A. Chirkunov, I.A. Arkhipushkin, L.P. Kazanskii and N.P. Andreeva, Protecting aluminum from atmospheric corrosion via surface hydrophobization with stearic acid and trialkoxysilanes, *Russ. J. Phys. Chem. A*, 2018, **92**, 621–629. doi: [10.1134/S0036024418040155](https://doi.org/10.1134/S0036024418040155)
9. A.M. Semiletov, A.A. Kudelina and Yu.I. Kuznetsov, New prospects in the application of superhydrophobic coatings and corrosion inhibitors, *Int. J. Corros. Scale Inhib.*, 2022, **11**, no. 3, 1388–1400. doi: [10.17675/2305-6894-2022-11-3-28](https://doi.org/10.17675/2305-6894-2022-11-3-28)
10. C. Esteves, Self-healing functional surfaces, *Adv. Mater. Interfaces*, 2018, **5**, no. 17, 1800293. doi: [10.1002/admi.201800293](https://doi.org/10.1002/admi.201800293)
11. L.E. Tsygankova and M. Vigdorowitsch, Anti-corrosion effectiveness of superhydrophobic coatings on metals. Overview, *Int. J. Corros. Scale Inhib.*, 2022, **11**, no. 3, 889–940. doi: [10.17675/2305-6894-2022-11-3-2](https://doi.org/10.17675/2305-6894-2022-11-3-2)
12. V.I. Vigdorovich, L.E. Tsygankova, A.M. Emel'yanenko, M.N. Uryadnikova and E.Yu. Shel, The effect of superhydrophobic coating on the electrochemical behavior of carbon steel in chloride and hydrogen sulfide–chloride environments, *Int. J. Corros. Scale Inhib.*, 2020, **9**, no. 1, 171–181. doi: [10.17675/2305-6894-2020-10-1-10](https://doi.org/10.17675/2305-6894-2020-10-1-10)
13. Y. Lin, H. Chen, G. Wang and A. Liu, Recent progress in preparation and anti-icing applications of superhydrophobic coatings. *Coatings*, 2018, **8**, no. 6, 208. doi: [10.3390/coatings8060208](https://doi.org/10.3390/coatings8060208)
14. S. Ozbay, C. Yuceel and H.Y. Erbil, Improved icephobic properties on surfaces with a hydrophilic self-lubricating liquid, *ACS Appl. Mater. Interfaces*, 2015, **7**, no. 39, 22067–22077. doi: [10.1021/acsami.5b07265](https://doi.org/10.1021/acsami.5b07265)
15. G.V. Redkina, A.S. Sergienko and Yu.I. Kuznetsov, Hydrophobic and anticorrosion properties of thin phosphonate – siloxane films formed on a laser textured zinc surface, *Int. J. Corros. Scale Inhib.*, 2020, **9**, no. 4, 1550–1563. doi: [10.17675/2305-6894-2020-9-4-23](https://doi.org/10.17675/2305-6894-2020-9-4-23)
16. K.R. Khedir, G.K. Kannarpady, C. Ryerson and A.S. Birisa, An outlook on tunable superhydrophobic nanostructural surfaces and their possible impact on ice mitigation, *Prog. Org. Coat.*, 2017, **112**, 304–318. doi: [10.1016/j.porgcoat.2017.05.019](https://doi.org/10.1016/j.porgcoat.2017.05.019)
17. K.A. Emelyanenko, A.G. Domantovsky, E.V. Chulkova, A.M. Emelyanenko and L.B. Boinovich, Thermally Induced Gradient of Properties on a Superhydrophobic Magnesium Alloy Surface, *Metals*, 2021, **11**, no. 1, 41. doi: [10.3390/met11010041](https://doi.org/10.3390/met11010041)
18. K. Golovin, M. Boban, J.M. Mabry and A. Tuteja Designing self-healing superhydrophobic surfaces with exceptional mechanical durability, *ACS Appl. Mater. Interfaces*, 2017, **9**, no. 12, 11212–11223. doi: [10.1021/acsami.6b15491](https://doi.org/10.1021/acsami.6b15491)



19. P. Nguyen-Tri, H.N. Tran, C.O. Plamondon, D.V.N. Vo, S. Nanda, A. Mishra, H.P. Chao and A.K. Bajpai, Recent progress in the preparation, properties and applications of superhydrophobic nano-based coatings and surfaces: A review, *Prog. Org. Coat.*, 2019, **132**, 235–256. doi: [10.1016/j.porgcoat.2019.03.042](https://doi.org/10.1016/j.porgcoat.2019.03.042)
20. T.B. Nguyen, S. Park and H. Lim, Effects of morphology parameters on anti-icing performance in superhydrophobic surfaces, *Appl. Surf. Sci.*, 2018, **435**, 585–591. doi: [10.1016/j.apsusc.2017.11.137](https://doi.org/10.1016/j.apsusc.2017.11.137)
21. L.B. Boinovich, E.B. Modin, A.R. Sayfutdinova, K.A. Emelyanenko, A.L. Vasiliev and A.M. Emelyanenko, Combination of Functional Nanoengineering and Nanosecond Laser Texturing for Design of Superhydrophobic Aluminum Alloy with Exceptional Mechanical and Chemical Properties, *Acs Nano*, 2017, **11**, no. 10, 10113–10123. doi: [10.1021/acsnano.7b04634](https://doi.org/10.1021/acsnano.7b04634)
22. J. Zhu, A novel fabrication of superhydrophobic surfaces on aluminum substrate, *Appl. Surf. Sci.*, 2018, **447**, 363–367. doi: [10.1016/j.apsusc.2018.04.014](https://doi.org/10.1016/j.apsusc.2018.04.014)
23. S. Zheng, C. Li, Q. Fu, W. Hu, T. Xiang, Q. Wang, M. Du, X. Liu and Z. Chen, Development of stable superhydrophobic coatings on aluminum surface for corrosion-resistant, self-cleaning, and anti-icing applications, *Mater. Des.*, 2016, **93**, 261–270. doi: [10.1016/j.matdes.2015.12.155](https://doi.org/10.1016/j.matdes.2015.12.155)
24. Z. Lu, P. Wang and D. Zhang, Super-hydrophobic film fabricated on aluminium surface as a barrier to atmospheric corrosion in a marine environment, *Corros. Sci.*, 2015, **91**, 287–296. doi: [10.1016/j.corsci.2014.11.029](https://doi.org/10.1016/j.corsci.2014.11.029)
25. S. Czyzyk, A. Dotan, H. Dodiuk and S. Kenig, Processing effects on the kinetics morphology and properties of hybrid sol-gel superhydrophobic coatings, *Prog. Org. Coat.*, 2020, **140**, 105501. doi: [10.1016/j.porgcoat.2019.105501](https://doi.org/10.1016/j.porgcoat.2019.105501)
26. M. Ruan, J.W. Wang, Q.L. Liu, F.M. Ma, Z.L. Yu, W. Feng and Y. Chen, Superhydrophobic and anti-icing properties of sol-gel prepared alumina coatings, *Russ. J. Non-Ferrous Met.*, 2016, **57**, 638–645. doi: [10.3103/S1067821216060122](https://doi.org/10.3103/S1067821216060122)
27. S. Czyzyk, A. Dotan, H. Dodiuk and S. Kenig, Easy-to-Clean Superhydrophobic Coatings Based on Sol-Gel Technology: A Critical Review, *Rev. Adhes. Adhes.*, 2017, **5**, 325–360.
28. K.A. Emelyanenko, A.G. Domantovsky, E.V. Chulkova, A.M. Emelyanenko and L.B. Boinovich, Thermally Induced Gradient of Properties on a Superhydrophobic Magnesium Alloy Surface, *Metals*, 2021, **11**, no. 1, 41. doi: [10.3390/met11010041](https://doi.org/10.3390/met11010041)
29. A. Volpe, C. Gaudioso and A. Ancona, Laser Fabrication of Anti-Icing Surfaces: A Review, *Materials*, 2020, **13**, no. 24, 5692. doi: [10.3390/ma13245692](https://doi.org/10.3390/ma13245692)
30. Sh. Zheng, Ch. Li, Yu. Zhang, T. Xiang, Y. Cao, Q. Li and Zh. Chen, A General Strategy towards Superhydrophobic Self-Cleaning and Anti-Corrosion Metallic Surfaces: An Example with Aluminum Alloy, *Coatings*, 2021, **11**, no. 7, 788. doi: [10.3390/coatings11070788](https://doi.org/10.3390/coatings11070788)



31. S. Mokhtari, F. Karimzadeh, M.H. Abbasi and K. Raeissi, Development of superhydrophobic surface on Al 6061 by anodizing and the evaluation of its corrosion behavior, *Surf. Coat. Technol.*, 2017, **324**, 99–105. doi: [10.1016/j.surfcoat.2017.05.060](https://doi.org/10.1016/j.surfcoat.2017.05.060)
32. L. Zhao, Q. Liu, R. Gao, J. Wang, W. Yang and L. Liu, One – step method for the fabrication of superhydrophobic surface on magnesium alloy and its corrosion protection, antifouling performance, *Corros. Sci.*, 2014, **80**, 177–183. doi: [10.1016/j.corsci.2013.11.026](https://doi.org/10.1016/j.corsci.2013.11.026)
33. T. Abohalkuma, F. Shawish and J. Telegdi, Phosphonic acid derivatives used in self assembled layers against metal corrosion, *Int. J. Corros. Scale Inhib.*, 2014, **3**, no. 3, 151–159. doi: [10.17675/2305-6894-2014-3-3-151-159](https://doi.org/10.17675/2305-6894-2014-3-3-151-159)
34. A.A. Abrashov, N.S. Grigoryan, T.A. Vagramyan, M.A. Simonova, V.S. Miroshnikov and I.A. Arkhipushkin, Surface passivation of 5556 aluminum alloy in solutions based on cerium nitrate, *Int. J. Corros. Scale Inhib.*, 2021, **10**, no. 1, 132–144. doi: [10.17675/2305-6894-2021-10-1-8](https://doi.org/10.17675/2305-6894-2021-10-1-8)
35. E. McCafferty, Validation of corrosion rates measured by the Tafel extrapolation method, *Corros. Sci.*, 2005, **47**, no. 12, 3202–3215. doi: [10.1016/j.corsci.2005.05.046](https://doi.org/10.1016/j.corsci.2005.05.046)
36. ASTM F735-17, *Standard Test Method for Abrasion Resistance of Transparent Plastics and Coatings Using the Oscillating Sand Method*, ASTM International, West Conshohocken, PA, USA, 2017.
37. A. Abrashov, N. Grigoryan, Y. Korshak, T. Vagramyan, O. Grafov and Y. Mezhev, Regularities of the Formation of a Green Superhydrophobic Protective Coating on an Aluminum Alloy after Surface Modification with Stearic Acid Solutions, *Metals*, 2021, **11**, no. 11, 1718. doi: [10.3390/met11111718](https://doi.org/10.3390/met11111718)
38. A.A. Abrashov, N.S. Grigoryan, Y.V. Tolmachev and A.N. Serov, Environmentally friendly solution of hydrophobization of the 5556 alloy based on stearic acid and dimethyl sulfoxide, *Tsvetnye Metally (Non-Ferrous Metals)*, 2021, no. 10, 37–42 (in Russian). doi: [10.17580/tsm.2021.10.05](https://doi.org/10.17580/tsm.2021.10.05)

